RSC Advances

ROYAL SOCIETY OF CHEMISTRY

www.rsc.org/advances

Journal Name

ARTICLE

Polymer-based composites with improved energy density and dielectric constant by monoaxial hot-stretching for organic film capacitors application

Received 00th January 20xx,
Accepted 00th January 20xx

DOI: 10.1039/x0xx00000x

www.rsc.org/

Xu Huang,[a] Kai Wang[b] , Kun Jia[a] and Xiaobo Liu *[a]

Randomly oriented multiwalled carbon nanotubes (MWCNT)/polyarylene ether nitriles (PEN) composite films were prepared by solution casting method. The as-prepared films were then under monoaxial hot-stretching in the oven to enhance their orientations and crystallinities. Results showed that hot-stretching process enhanced the mechanical and thermal properties significantly. The development of electrical conducting pathways during the monoaxial hot-stretching of MWCNT/PEN composite films was studied. Since the content of MWCNTs filler is close to the percolation threshold, ca. 6 wt%, the dielectric properties, electrical conductivity, breakdown strength and energy density were found to be very sensitive to the stretch ratio. The electrical conductivity of composites with 50% stretch ratio increased from $5.2*10^{-5}$ S·cm^{-1} to $1.6*10^{-4}$ S·cm^{-1} (1 kHz). Besides, dielectric constant of composites with 50% stretch ratio increases amazingly from 378.0 to 1298.1 (100 Hz). Mostly importantly, the composites with 50% stretch ratio compensates some dielectric constant with breakdown strength, and finally, the energy density of the composites with 50% stretch ratio increases by about 40%, from 2.51 to 3.50 J/cm^3, which has huge potential to be used as organic film capacitors.

Introduction

Recently, multiwalled carbon nanotubes (MWCNTs) is well known for its intriguing properties such as mechanical[1,2],thermal[3]and electrical[4] conductive properties. Particularly, the extraordinary mechanical and electrical properties make them ideal reinforcing materials for polymer based composites[5]. Good dispersion state and orientation are two key issues to realize the reinforcement to polymer composites[6-8]. Besides, MWCNTs can provide the potential of the nucleation site for the crystal polymers. Polyarylene ether nitriles(PEN), as a special thermoplastic engineering material, possesses various outstanding properties, including excellent mechanical properties, high thermal stability, radiation resistance and chemical inertia nature, etc[9-11]. These characteristics make it a good candidate to be used in industrial, automotive and outer space fields encountered with high temperature or high radiation exposure[12-14]. Many studies have reported that MWCNTs can be well dispersed in the polymer matrix and act as a nucleation site for crystal polymer[15-19]. Generally, oriented CNTs in polymer matrix can be achieved by magnetic field[20], or by mechanical stretch[21-23]. In terms of the stretch methods, there are cold stretch, hot stretch, monoaxial stretch[24,25] and biaxial stretch[26]. Some former studies focused on the orientation of carbon nanotubes in matrix and its effect on morphological and mechanical properties of composites. However, few studies dealt with the electrical properties of the oriented MWCNTs in polymer matrix during mechanical stretch process. In this study, MWCNTs/PEN composite films were prepared by solution casting method. Then, the as-prepared films were under monoaxial hot-stretching in the oven at a temperature slightly below the melting temperature. The stretch ratios corresponded to 50%, 100%,200%, and 400%, respectively. The main goal of this study is to reveal the intrinsic relationship between mechanical stretch and mechanical, thermal, and electrical properties of the composites.

Experimental

Materials

MWCNTs (purity 98 wt%) were about 20 nm in outer diameter and 15-20 μm in length, purchased from Chengdu Organic Chemicals Co., Ltd., Chinese Academy of Science, which was used without any purification. Toluene (99%) was purchased from Chengdu Kelong chemical Reagent Co., Ltd., Chengdu, China. *N*-methylpyrrolidone (NMP, purity 99%) was purchased from Tianjin Bodi Chemical Holding Co., Ltd., Tianjin, China. Diphenol(DP, 99%) and 2,6-dichlorobenzonitrile(DCBN) were bought from Shanghai Chemical

[a]*Research Branch of Advanced Functional Materials, Institute of Microelectronic & Solid State Electronic, High-Temperature Resistant Polymers and Composites Key Laboratory of Sichuan Province, University of Electronic Science & Technology of China, Chengdu 610054, P.R. China.*
[b] *College of Polymer Science and Polymer Engineering, University of Akron, Akron, Ohio 44325, United States;*
**Corresponding author: Xiaobo Liu( ) fax/tel:+86-028-83207326;*
E-mail address: liuxb@uestc.edu.cn

Reagent Co., Ltd., shanghai, China. Anhydrous potassium carbonate (K_2CO_3, AR) was bought from Xilong Chemical Co., Ltd., Guangdong, China. Polyarylene ether nitriles (PEN) was synthesized and purified in our laboratory.

Synthesis of polyarylene ether nitriles

Polyarylene ether nitriles (PEN) was synthesized via nucleophilic aromatic substitution polymerization. During the reaction, DP (0.4 mol, 75.2 g), and DCBN (0.4 mol, 68.8 g) were mixed in a 500 mL three-necked round-bottom flask equipped with a Dean Stark trap combined with a condenser, a thermometer and a mechanical stirrer. Firstly, 50 mL toluene and 150 mL NMP were added into the flask orderly. Then, anhydrous K_2CO_3 (0.8 mol, 66.0 g) was added into the three-necked round-bottom flask in several times. After the water-toluene azeotrope distilled off, the reaction mixture was heated to 200 ℃ and kept at 200 ℃ for approximately 4 h. Afterwards, the mixture was poured into 1000 mL of deionized water and smashed by a muller. After that, the mixture was poured into 1000 mL of dilute HCl solution in order to remove the residuary catalyst K_2CO_3, and then rinsed byalcohol till the solvent and monomers were washed out completely. After being filtrated, it was dried at 100 ℃ overnight. The schematic diagram of the PEN was depicted in Fig. 1.

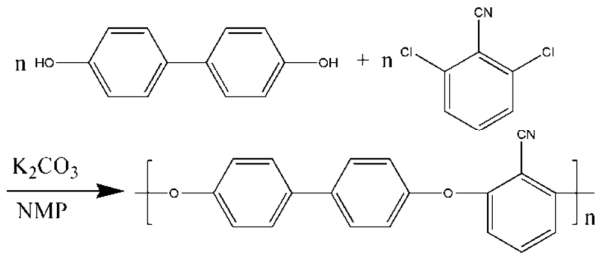

Fig.1 Schematic diagram to synthesize crystalline PEN.

Preparation of MWCNT/PEN composite films

MWCNTs/PEN composite films were obtained by solution casting method after continuous ultrasonic dispersion. Firstly, a certain amount of MWCNTs powder were gradually added into a certain volume of NMP solvent, and treated for 2 h by ultrasonic waves (ultrasonic frequency: 40 kHz; electric power: 200 W) to make sure that the MWCNTs were homogeneously dispersed. Meanwhile, a certain amount of PEN and NMP solvent was slowly added into a three-necked bottle which was equipped with a refluence condenser, a mechanic blender and a heater. PEN was gradually dissolved in NMP solvent and formed a transparent PEN solution as the temperature raised up. Then, MWCNTs suspension was slowly added into the PEN solution. Then, the MWCNTs/PEN suspension was treated with ultrasonic wave for another 1 h at 80 ℃. Finally, the suspension was cast onto a clean horizontal glass plate and dried in an oven at 80 ℃, 100 ℃, 120 ℃, 140 ℃, 160 ℃, 180 ℃and200 ℃ each for 1 h. Subsequently, the films were cooled naturally to room temperature in the oven. Finally, the MWCNTs/PEN composite films were obtained. The mass fraction of MWCNTs in the PEN matrix was fixed at 6 wt%. The average thickness of the films was approximately 0.06 mm.

Monoaxial hot-stretching of MWCNT/PEN composite films

Firstly, MWCNT/PEN composite films were cut into standard strips (1 cm×15 cm), then, as shown in Fig. 2, clamps were used to nip both ends of the strips. Thus, the upside of the sample can be hung in the high temperature oven. The clamps were adjusted to make sure that distance of sample between the two clamps is 10 cm. After that, the upside of the samples were hung in the oven, a balancing weight of 100 g was added to the downside of each sample. Most importantly, the stretching ratios of the four samples were controlled by the distance between the downside of the samples and the bottom of the oven. Bricks with different height were added to the bottom of the oven to change the distance between the downside of the sample and top of the bricks. The distance was 5 cm, 10 cm, 20 cm, and 40 cm, respectively. Then, these strips were mechanically stretched by applying a constant load of 100 g at 350 °C until the strips were stretched to the expected length. When temperature of the oven increased, the polymer chains started to slide, the 100 g weight would fall down to upside of the bricks together with the samples. After this procedure, the length of each stripe-like sample would be stretched to 15 cm, 20 cm, 30 cm, and 50 cm, respectively. The increment of the specimen was 5 cm, 10 cm, 20 cm, and 40 cm, respectively. That is to say, the stretching ratio of the four samples should be 50%, 100%, 200% and 400% (length increment divide by initial length), respectively. After the desired stretch ratios were obtained, the specimens were cooled down to room temperature and then the load was released. It was found that shape of the obtained hot-stretching strips can stay steady and will not recover. Besides, as-prepared MWCNT/PEN composite film without any stretch treatment was used for comparison.

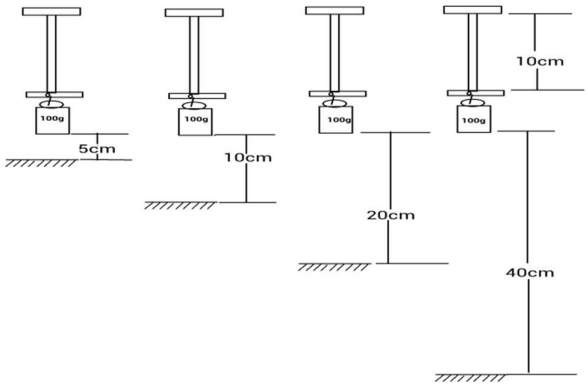

Fig. 2 Schematic diagram to fabricate monoaxial hot-stretching MWCNT/PEN composite films.

Characterizations

X-ray diffraction (XRD) analysis was carried out in a Rigaku RINT2400 X-ray diffractometer with Cu Kα radiation. The cross section microstructures of the films were observed with scanning electron microscope (SEM, JEOL, JSM-5900 LV), and the samples were coated with a thin layer of gold before

testing. Differential scanning calorimetry (DSC) analysis of the nanocomposite films was carried out on a TA Instrument DSC Q100 under nitrogen atmosphere from room temperature to 300 ℃ at a heating rate of 10 ℃/min. Mechanical properties of the pure and nanocomposite films were measured by employing a SANS CMT6104 Series Desktop Electromechanical Universal Testing Machine. The films were cut into stripes (120 mm in length, 10 mm in width) for testing, and the reported values were calculated as average values by five samples for each film(stretching speed 5 mm/min).

Dielectric properties of the stretched MWCNTs/PEN films were tested by a TH 2819A precision LCR meter (Tong hui Electronic Co., Ltd.). The films were cut into small pieces of samples (10 ×10 mm), and both sides of the samples were coated with a thin layer of conductive silver paste to form a plate capacitor. The dielectric properties experiments were carried out at different frequencies ranging from 100 Hz to 100 kHz at room temperature with 40% humidity. The dielectric constant and electrical conductivity were calculated through equations listed below. The dielectric constant (ε_r) is expressed as

$$\varepsilon_r = \frac{C\,d}{S\,\varepsilon_0} \qquad (1)$$

where C is the capacitance of the samples; d is the thickness of the samples; S is the area of the electrode; $\varepsilon_0 = 8.85 \times 10^{-12}$ F/m is the vacuum dielectric constant. The electrical conductivity (σ) is shown as

$$\sigma = \frac{I\,d}{U\,S} \qquad (2)$$

where U is the voltage; I is the electric current; S is the area of the electrode and d is the thickness of the samples. Volume resistivity (ρ) is the inverse of electrical conductivity ($\rho=\sigma^{-1}$).

Results and discussions

Morphology before and after the monoaxial hot-stretching

The dispersion state and alignment of the MWCNTs in the PEN matrix was characterized by SEM. Fig.3a and b showed the microstructure evolution of composite films with 6 wt% MWCNT/PEN before and after hot-stretching, respectively. Why do we choose 6 wt% filler loading? Former researches showed that for a specimen filled with MWCNTs well near the percolation threshold[27], the decrease in number of MWCNT-MWCNT direct contacts was more severe than for a specimen far below or above percolation threshold, on condition that they were subjected to the same stretch ratio. As can be seen, when the MWCNT/PEN composite films is subjected to hot-stretching, the original microstructure of the composite film started to change, thereby influencing the total number of MWCNT-MWCNT direct contacts. This is due to the originally random orientation of MWCNTs becoming more ordered after unidirection stretch. The stretch ratio of the specimen shown in Fig. 3b is about 200%. The microstructures of the specimen were observed after being coated by a layer of gold so as to obtain better observation. By comparing the pristine composite film (shown in Fig. 3a) with the stretched film (shown in Fig. 3b), it can be concluded that initially random oriented carbon nanotubes embedded in the PEN matrix become aligned and paralleled with the direction of stretch. As can be seen, aligned MWCNTs were achieved macroscopically and widely through the stretching process. It is deemed that the total number of MWCNT-MWCNT direct contacts decreases as the carbon nanotubes become more and more paralleled, causing an decrease in electrical conductivity. As a result, the electrical conductivity of the specimen can be controlled by varying the stretch ratio of the specimen.

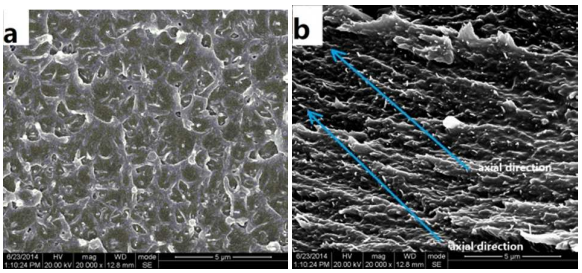

(a) Before hot-stretching (b)After hot-stretching

Fig. 3 Microstructure of 6wt% MWCNT/PEN composite films before and after hot-stretching.

XRD spectrum of the hot-stretching MWCNT/PEN composite films

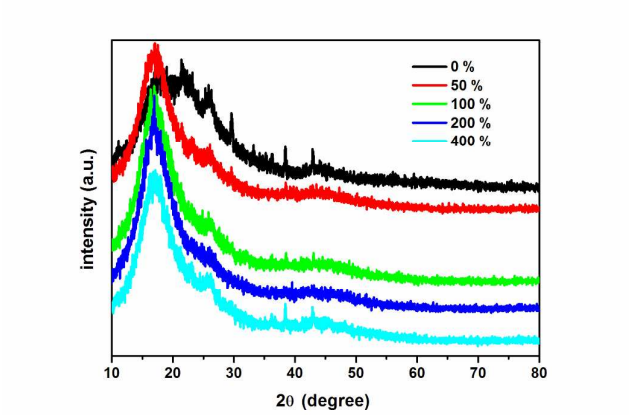

Fig. 4 Wide-angle XRD patterns of pristine and hot-stretching MWCNT/PEN composite films with different stretch ratios.

The wide-angle X-ray diffraction patterns were collected from both the non-stretched film and specimens with different stretch ratios (the load was released). In order to investigate the effect of hot stretch on the crystal structures of stretched MWCNT/PEN composites, Wide-angle XRD patterns of specimens with measuring angles from 10° to 80° were obtained. As shown in Fig. 4, the non-stretchedspecimen showed a very board peak composed by several overlapped peaks at 2θ=18°, 24° and 26°, which is in accordance with previous reports[13].In contrast, the diffraction pattern of the stretched specimens showed a sharper and stronger peak at about 2θ = 18°. This indicated that some of the polymer crystal structures disappeared or reduced after hot stretch process and other crystal structures become more stable and perfect.

And it also can be found that there exists very weak peaks at about 2θ = 26°, corresponding to the diffraction peak of MWCNTs[28].

Table1 Crystallinity and crystal size of pristine and hot-stretching MWCNT/PEN composite films calculated from *X*-ray diffraction.

Stretch ratio	0%	50%	100%	200%	400%
Crystallinity (%)	11.5	11.0	10.5	9.2	8.7
Crystal size (nm)	30	28	26	21	19

Table 1 presented the values of the percent crystallinity and the average crystal sizes for MWCNT/PEN composites. We employed the Jade software to roughly calculate the percent crystallinity and the average crystal sizes.The original file was open by Jade software, then we use profile fitting menu for peak decomposition. We have fitted curves several times to make sure that the residual error of fit is less than 4% (R<4%) in the fitting process. After the baseline is calibrated , crystallinity of the sample is obtained via clicking the report menu (then click the sub-menu" peak file report"). The detailed crystallinity value will obtained.The crystallinity of the hot-stretched specimens decreased from 11.5% gradually to 8.7% in comparison with those of non-stretched specimen. Besides, the crystal size also decreased about 37%. The decrease in crystal size can be attributed to the destruction of imperfect crystals caused by high temperature. The crystals left in the composites were those with more stable and perfect crystal structures.

Thermal properties of the hot-stretching MWCNT/PEN composite films

Additional structural information can be revealed by thermal behavior of the stretched specimens, as measured by DSC and shown in Fig. 5. It was reported that the stretch process will affect the crystallization behavior of the crystal structure of the MWCNT/PEN composites. Fig.5 showed the melting endotherms of monoaxial hot-stretching composites with 6wt % MWCNTs. Obvious changes in the melting curves occurred as the stretch ratio was increased. Besides, the heat of fusion (ΔH_m) and melting point (T_m) were summarized in Table 2. As the composite was monoaxially stretched, a slight increase in melting temperature was detected. For non-stretched specimen, the melting point of the was around 352 ℃, As the composite was monoaxially stretched to 50%, 100%, 200%, and 400%, the melting point increased to 368 ℃, 374 ℃, 376 ℃, and 377 ℃, respectively. However, the overall heat of fusion was decreased from 44.7 J/g gradually to 18.6 J/g, as shown in Table 2. On the basis of the heat of fusion of 100% crystalline (ΔH_m) original MWCNT/PEN, the degree of crystallinity of hot-stretching MWCNT/PEN composites were determined by the ratio of the ΔH_m for the hot-stretching specimens to that of 100 % crystallized MWCNT/PEN. Even though the ΔH_m of 100 % crystalline MWCNT/PEN is uncertain. It can be inferred that the crystallinity of hot-stretching MWCNT/PEN composites were decreased as the stretch ratio increases, which was in accordance with the results of the XRD analysis. The increase of melting point may be caused by two main factors: on the one hand, the defective crystalline zones changed to amorphous zones; on the other hand, much more stabilized crystal structures formed during the hot stretch process. Usually, slow stretch speed would increase the crystallinity of the polymer, as reported in former literature[29]. However, in this case, the stretch speed was too fast and out of control, so the polymer chains do not have enough time to form typical lamellae crystals. That is why the melting point of the obtained MWCNT/PEN composites increases, while the crystallinity decreases.

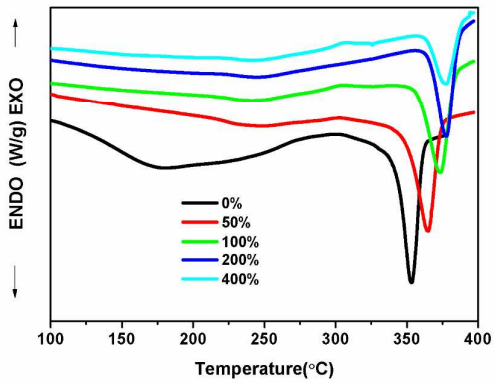

Fig. 5DSC curves of hot-stretching MWCNT/PEN composite films with different stretch ratios.

Table 2 Thermal properties of the MWCNT/PEN hot-stretching composite films

Stretch ratio	0%	50%	100%	200%	400%
ΔH_m (J/g)	44.7	38.2	33.5	27.1	18.6
T_m (℃)	352	368	374	376	377

Mechanical properties of the hot-stretching MWCNT/PEN composite films

The tensile strength and tensile modulus of the MWCNT/PEN composite films with different stretch ratios were shown in Fig. 6. As expected, higher stretch ratios leaded to higher tensile modulus of the composite films. The pristine MWCNT/PEN specimen exhibited a tensile strength of 84 MPa. While the tensile strength of the composite films with stretch ratios of 50%, 100%, 200%, and 400% were improved to 150, 185, 291, and 313 MPa, respectively, corresponding to 79%, 120%, 246%, and 271% increment over those of the pristine composite films. The tensile modulus of MWCNT/PEN composite films without hot-stretching was 2805 MPa. This was increased to 3156, 3867, 3623, and 3885 MPa with four different stretch ratios of 50%, 100%, 200% and 400%, respectively, which corresponded

to 13%, 38%, 29%, and 39% increment over those of the non-stretched MWCNT/PEN composites. These results were in consistent with former reports in the literatures[30]. SEM image showed that hot-stretching lead to improved alignment of the carbon nanotubes in the PEN matrix. With increasing stretch ratio, more nanotubes were aligned and re-dispersed since the polymer start to orient during the hot-stretching process. Besides, former reports showed that the crystalline polymer tends to recrystallize during the hot-stretching process[31]. Through enhanced alignment of MWCNTs and better crystallization of PEN polymer, the tensile mechanical properties of the hot-stretching MWCNT/PEN composites were significantly improved.

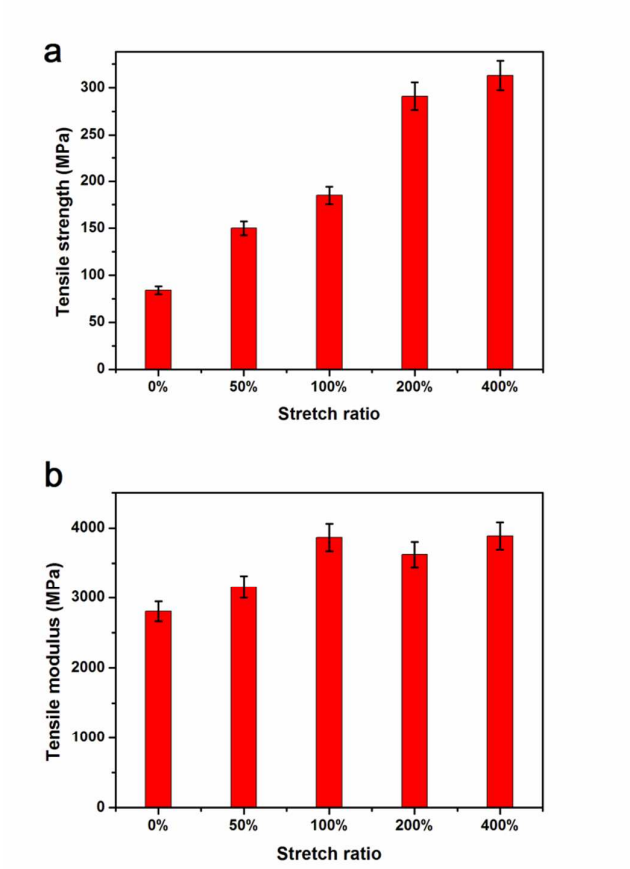

Fig. 6 Tensile strength (a) and tensile modulus (b) of the hot-stretching MWCNT/PEN composite filmsas a function of stretch ratio.

Electrical properties of the hot-stretching MWCNT/PEN composite films

Dielectric constant (ε_r), dielectric loss ($tan\delta$), volume resistivity (ρ), electrical conductivity (σ), breakdown strength (E_b), and energy density (U) of the hot-stretching MWCNT/PEN composites were investigated in detail.

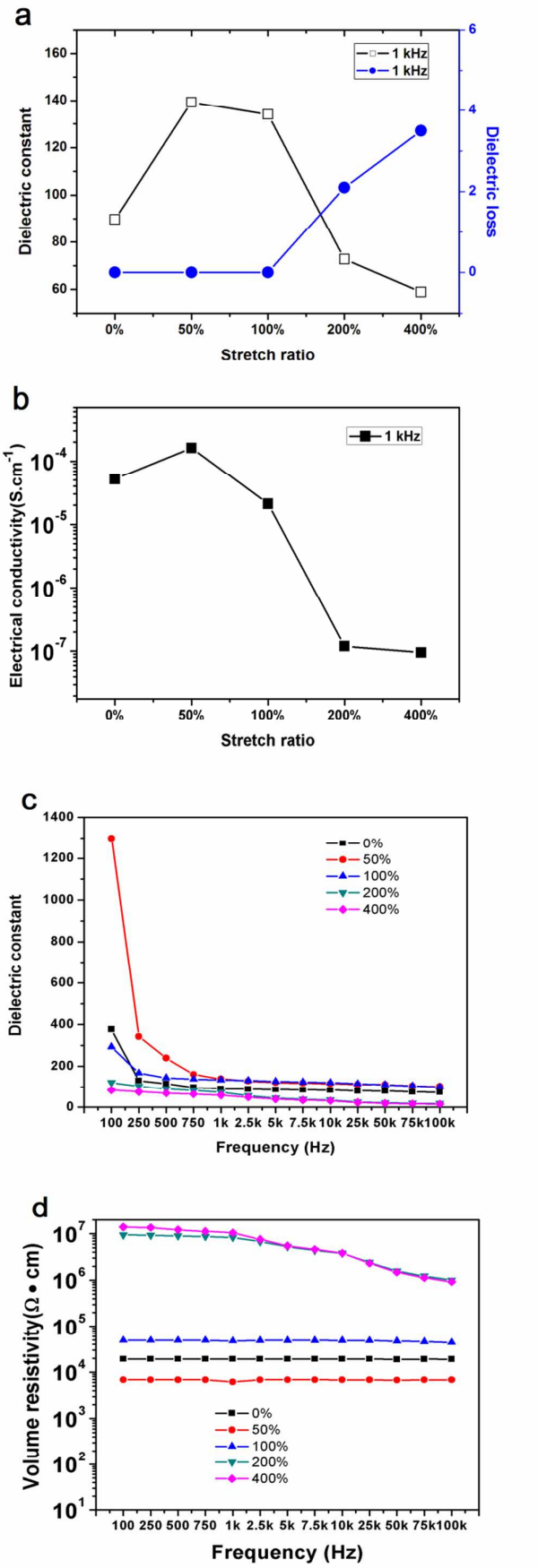

Fig.7(a)Dielectric properties and (b) electrical conductivity of the hot-stretching MWCNT/PEN composite as a function of stretch ratio at 1 kHz.(c) dielectric constant and(d) volume resistivity of the hot-stretching MWCNT/PEN composite films as a function of frequency.

The dielectric constant and dielectric loss measured at 1 kHz was shown in Fig. 7a. As can be seen, the dielectric constant increased obviously as the stretch ratio reached 50%, indicating the beginning of alignment and orientation of MWCNTs. This could be attributed to the conductive pathways changes and microcapacitors formation during the stretch process[32].

Dielectric constant of composites with 50% stretch ratio increased amazingly from 378.0 to 1298.1 (100 Hz). Most of the MWCNT-MWCNT contacts disappear and only a small part remained as the stretch ratio reached 200%. That was why the ε_r decreases abruptly, smaller than that of the pristine one. Finally, as the stretch ratio increased to 400%, there were fewer and fewer MWCNT-MWCNT contacts and conductive pathways broke up, as a result, the dielectric constant reduced. Dielectric loss provided another supplementary proof for the change of the inner conductive structure. Since there were conductive pathways in the MWCNT/PEN system, so, *tanδ* for specimen with 0%, 50% and 100% stretch ratio were beyond test range. When the conductive pathways in specimen with 200% and 400% stretch ratio disappeared, the *tanδ* was measurable.The electrical conductivity of the specimens with different ratios at 1 kHz was presented in Fig. 7b. The electrical conductivity of composites with 50% stretch ratio increased from$5.2*10^{-5}$ $S{\cdot}cm^{-1}$to$1.6*10^{-4}$ $S{\cdot}cm^{-1}$. This increase in electrical conductivity is possibly due to the alignment of the MWCNTs. When more MWCNTs started to align with the stretch direction, more conductive pathways would be formed, thus, the conductivity increases. However, when the stretch ratio reached 100%, MWCNT-MWCNT contacts started to reduce, resulting in decrease in electrical conductivity of the specimen.

Figure 7c and d showed the dielectric constant and volume resistivity of the hot-stretching composite films with different stretch ratios as a function of frequency from 100 Hz to 100 kHz. As shown in Fig. 7c, for MWCNT/PEN composite with 50% and 100% stretch ratio, the ε_r showed a increment.For MWCNT/PEN composites with 100% and 200% stretch ratio, theε_r decreased.The phenomenon was observed under different frequency range. The ε_r shows a larger value under low frequency range and a smaller value under higher frequency, which was due to the fact that the speed of polarization couldn't catch up with the change speed of field.

Table 3 showed the value of $tan\delta$ of MWCNT/PEN composite films with different stretch ratios and frequencies. As the filler content is near the percolation threshold, *tanδ* is beyond measurement range for pristine MWCNT/PEN composites. For composite with 100% stretch ratio, the dielectric constant under higher frequency become smaller and measurable. This is ascribed to the fact thatorientational polarization couldn't catch up with the change speed of field, consuming less energy due to smaller friction during the orientation process. For composites with 200% and 400% stretch ratios, the *tanδ* is measurable since the distance between the fillers was increase during the stretching process.

Table 3 Dielectric loss of the hot-stretching MWCNT/PEN composite films under different frequencies.

Hz	0%	50%	100%	200%	400%
100	-	-	-	-	-
250	-	-	-	5.00	-
500	-	-	-	3.10	5.80
750	-	-	-	2.40	4.20
1k	-	-	-	2.10	3.50
2.5k	-	-	-	1.40	1.90
5k	-	-	-	1.10	1.40
7.5k	-	-	-	0.96	1.20
10k	-	-	-	0.89	1.08
25k	-	-	-	0.73	0.82
50k	-	-	6.80	0.62	0.68
75k	-	-	4.90	0.56	0.61
100k	-	-	3.90	0.52	0.56

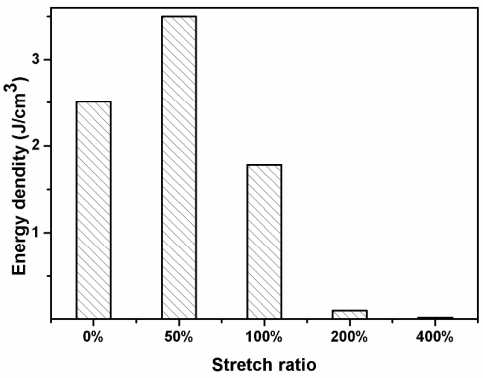

Fig. 8 Energy density of the MWCNT/PEN hot-stretching composite film as a function of stretch ratio.

The dielectric constant and breakdown strength of pristine and stretched MWCNT/PEN composite films were listed in Table 6. The energy density was calculated from equation 3 and was presented in Fig. 8. The energy density (*U*) of a capacitor is given by the following equation,

$$U = \frac{1}{2}\varepsilon_0\varepsilon_r E_b^2 \qquad (3)$$

where ε_r is the dielectric constant of the composite and $E_b$is the breakdown strength. As can be seen from Equation (3), two variables (dielectric constant and E_b) together determine the value of energy density. As the stretch ratio increased, the dielectric constant firstly increased a little and then decreased gradually, while the breakdown strength continue to reduce. It was clear that E_b had a stronger effect on the energy density of the specimen. So, it was presumed that the increment of *U* can only be obtained on condition of a slight decrease of E_b. The

calculated results proves that when the stretch ratio reaches 50%, the E_b is increasedby about 40%,from 2.51 to 3.50 J/cm^3. After this turning point, the energy density of the composites decreases dramatically since there is a power law between the energy density and breakdown strength. This is the result of sharp increase in dielectric constant and little decrease in breakdown strength. Therefore, hot-stretching process is an effective method to improve the energy density of the MWCNT/PEN composites.

Table 4 Breakdown strength and energy density of the MWCNT/PEN hot-stretching composite films.

Stretch ratio	0%	50%	100%	200%	400%
Dielectric constant, ε_r(at 1 kHz)	89.7	139.3	134.0	72.8	58.9
Breakdown strength , E_b(kV/mm)	79.6	75.4	54.8	17.8	8.9
Energy density, U (J/cm^3)	2.51	3.50	1.78	0.10	0.02

Intrinsic relationship between stretch ratio and conductive network.

Based on the above analysis, it can be inferred that the hot stretch process was accompanied with breakup of old conductive network and the rebuilding of new conductive pathway. The degree oforientation and the inner network of MWCNTs were mainly dependent on the stretch ratio and movability of polymer chains. A theoretical model was put forward (see Fig. 9) to explain the intrinsic structure change of the composites. As CNTs were dispersed and surrounded by PEN polymer matrix, they would move with both the amorphous chains and crystallite zones when the specimen is under stretch. Once the specimen was in the strain-hardening region, the chains in crystalline regions would become movable and align along the stretching direction, promoting the breakup of MWCNT aggregations and offering a chance to rebuild the conductive pathways. The stretch ratio was one of the vital factors determining the conductive network structure. When the stretch ratio reached 50%, part of the MWCNTs started to align with the stretch direction. This was still a conductive network since there were MWCNT-MWCNT contacts throughout the network. As the stretch ratio reached 100%, almost all of the MWCNTs had already aligned with the stretch orientation, and there were still conductive network throughout the system. However, in stage *d*, there were only partial MWCNT-MWCNT contacts left and the conductive pathways started to break up. In stage *e*, the MWCNTs started to depart from each other and conductive network broke up finally.

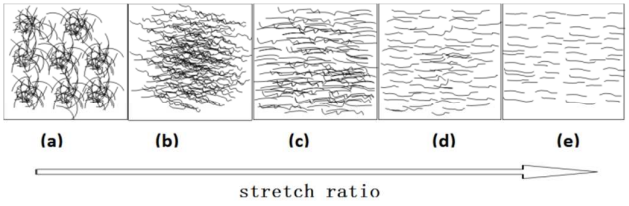

Fig. 9 Theoretical model of inner conductive network in MWCNT/PEN composites during monoaxial stretching: a, b, c, d, and e correspond to the stretch ratio of 0%, 50%, 100%, 200%, and 400%, respectively.

Conclusions

In the current research, monoaxial hot-stretching has proved to be an effective way to enhance the mechanical and thermal properties of MWCNT/PEN composites. Besides, the electrical properties are dependent on the stretch ratio, making it possible to modulate the electrical properties by adjusting the stretch ratios. In all, the following conclusions have been drawn.

(1) It was found that shape of the obtained hot-stretching strips can stay steady and will not recover because of the crystallinity of PEN.

(2) Tensile strength of the stretched composites increase from 84 MPa to 313 MPaas the stretch ratio gradually increases to 400%.

(3) Melting point of the stretched composites increases from 352℃to 377℃.

(4) XRD analysis shows that crystallinity and the size of crystallite decreases since some of the imperfect crystals and less stable were destroyed during the stretch process.

(5) Since content of MWCNTs in the composites is near the percolation threshold, the electrical properties are very sensitive to the stretch ratio. For example, the electrical conductivity of composites with 50% stretch ratio increased from 5.2*10^{-5} S·cm^{-1}to1.6*10^{-4}S·cm^{-1}(1kHz). Dielectric constant of composites with 50% stretch ratio increases from 89.7 to 139.3 (100 Hz). However, breakdown strength merely decreases from 79.6 to 75.4 (kV/mm). As a result, energy density of the composites with 50% stretch ratio increases from 2.51 to 3.50 J/cm^3, increases by approximately 40% than the one without hot-stretching.

(6) This simple methodology to improve the properties of polymer composites is expected to be applicable to other polymer-based composites.

Acknowledgements

The authors wish to thank for financial support of this work from the National Natural Science Foundation (Nos. 51173021, 51373028, 51403029), "863" National Major Program of High Technology (2012AA03A212),Ningbo Major (key) Science and Technology Research Plan (2013B06011) and South Wisdom Valley Innovative Research Team Program.

Notes and references

1 M. F. Yu, O. Lourie, M. J. Dyer, K. Moloni, T. F. Kelly, and R. S. Ruoff. Science 2000; 287(5453): 637-40
2 E.W. Wong, P.E. Sheehan, and C.M. Lieber. Science, 1997; 277(5334): 1971-5.
3 P. Miaudet, C. Bartholome, A. Derre. M. Maugey, G. Sigaud, C. Zakri, and P. Poulin, Polymer 2007; 48(14): 4068-74.
4 A. Javey, J. Guo, Q. Wang. M. Lundstrom, and H. Dai, Nature 2003; 424(6949): 654-7.
5 J.N. Coleman, U. Khan, W.J. Blau, and Y. K. Gun'ko, Carbon 2006; 44(9): 1624-52.
6 J.N. Coleman, U. Khan, and Y.K. Gun'ko, Advanced Materials 2006; 18(6): 689-706.
7 M. Moniruzzaman, and K. I. Winey, Macromolecules 2006; 39(16): 5194-205.

8 M. Xu, T. Zhang, B. Gu, J. Wu, and Q. Chen, Macromolecules 2006; 39(10): 3540-5.
9 X. Liu, R. Du, L. Hao, S. Wang, G. Cao, H. Jiang, Express Polym Lett2007; 1(8): 499-505.
10 Y. Zhan, X. Yang, F. Meng, R. Zhao, and X. Liu, Journal of Colloid and Interface Science 2011;363 (1): 98-104.
11 H. Tang, Z. Ma, J. Zhong, J. Yang, R. Zhao, and X. Liu, Colloids and Surfaces A 2011;384(1): 311-7.
12 Z. Pu, H. Tang, X. Huang, J. Yang, Y. Zhan, R. Zhao and X. Liu, Colloids and Surfaces A 2012; 415: 125-133.
13 P. Zheng, Z. Pu, W. Yang, , S. Shen, K. Jia, and X. Liu, Journal of Materials Science: Materials in Electronics, 2014; 25(9): 3833-9.
14 X. Huang, M. Feng, X. Liu, Polymer International 2014; 63(7): 1324-31.
15 M.S. Shaffer, A. H. Advanced Materials 1999; 11(11): 937-41.
16 M. Cadek, J. N. Coleman, K. P. Ryan, V. Nicolosi, G. Bister, A. Fonseca, and W. J. Blau, Nano Letters 2004; 4(2): 353-6.
17 J. N. Coleman, M. Cadek, R. Blake, V. Nicolosi, K. P. Ryan, C. Belton, and W. J. Blau, Advanced Functional Materials 2004; 14(8): 791-8.
18 M. Cadek, J. N. Coleman, V. Barron, K. Hedicke and W. J. Blau, Applied Physics Letters 2002; 81(27): 5123-5.
19 D. Blond, V. Barron, M.Ruether, K. P. Ryan, V. Nicolosi, W. J. Blau, and J. N. Coleman, Advanced Functional Materials 2006; 16(12): 1608-14.
20 G. Piao, F. Kimura, T. Takahashi, Y. Moritani, H. Awano, S. Nimori, and T. Kimura, Polymer journal 2007; 39(6): 589-92.
21 L. Jin, C. Bower, O. Zhou, Applied Physics Letters1998; 73(9): 1197-1199.
22 Y. Bin, M. Kitanaka, D. Zhu, and M. Matsuo, Macromolecules 2003; 36(16): 6213-9.
23 Y. Bin, A. Yamanaka, Q. Chen, Y. Xi, X. Jiang, and M. Matsuo, Polymer journal 2007; 39(6): 598-609.
24 T. Liu, and S. Kumar, Nano Letters 2003; 3(5): 647-50.
25 X. Zhang, T. Liu, T. V. Sreekumar, S. Kumar, V. C. Moore, R. H. Hauge, and R. E. Smalley, Nano Letters 2003; 3(9): 1285-1288.
26 X. Zhang, T. Liu, T. V. Sreekumar, S. Kumar, X. Hu, and K. Smith, Polymer 2004; 45(26): 8801.
27 X. L. Xie, Y. W. Mai, and X. P. Zhou, Mater Sci Eng: R 2005; 49(4): 89-112.
28 S.W. Lee, W.M. Sigmund, Chemical Communications 2003; (6): 780-1.
29 Y. Bin, M. Kitanaka, D. Zhu, and M. Matsuo, Macromolecules 2003; 36(16): 6213.
30 X. Zhao, and L. Ye, Composites Science and Technology 2011; 71(10): 1367-72.
31 Z. Song, X. Hou, L. Zhang, and S. Wu, Materials 2011; 4(4): 621-32.
32 S. H. Yao, J. K. Yuan, T. Zhou, Z. M. Dang, and J. Bai, The Journal of Physical Chemistry C 2011; 115(40): 20011-7.